Journal of ELECTRICAL ENGINEERING, VOL 70 (2019), NO6, 489–493

sciendo

PAPERS

Non-contact detection of impact damage in carbon fibre composites using a complementary split-ring resonator sensor

Zhen Li[*,], Tianqi Wang[*], Arthur Haigh[***], Zhaozong Meng[****], Ping Wang[*,**]**

In this paper, a new non-contact method for detection of impact damage in carbon fibre-reinforced polymer composites with a complementary split-ring resonator sensor is proposed. The resonance frequency is evaluated as an indicator of the presence of damage. The resonator is made on a printed circuit board, and in the experimental setup it is positioned close to the area of interest. Electromagnetic models are built, and from the resonant responses the appropriate frequency range used for the test is determined. The active sensing element in the resonator is found from the analysis of the magnetic field distribution. The parametric study performed shows that a larger frequency change occurs for a wider impacted region, which is of great use for practical applications. The proposed method is validated by the experimental results, where a frequency shift of 65 MHz was observed for a 0.36 mm deep dent.

K e y w o r d s: carbon fibre composites, impact damage, non-destructive detection, microwave sensor, complementary split-ring resonator, electromagnetic simulation

1 Introduction

Carbon fibre-reinforced polymer (CFRP) composites have been increasingly used in aerospace, automotive and marine structures year on year, owing to their superior stiffness and strength characteristics, good fatigue and corrosion resistance [1]. However, in the field carbon fibre composites remain vulnerable to impact, caused by objects and events such as hail stones, runway debris, collision with ground equipment, tool drops and bird strikes. The types of damage induced by impact include surface dents, delamination, matrix cracks and fibre breakage. And in many occasions, these happen internally and are hardly observed by visual inspection. Various non-destructive testing (NDT) techniques can be applied for damage detection, such as ultrasonic testing, acoustic emission, thermography, shearography, vibration testing, optical fibre sensing, guided waves (*eg* Lamb waves [2]) and digital image correlation (DIC). It is noted that each method has its advantages, disadvantages and fields of application [3, 4]. For example, in ultrasonics couplants are required, and the acoustic emission sensors shall be placed near the damage region. For thermography, the possibility of unwanted thermal damage caused during the inspection should be considered. In the setups of shearography and vibration testing techniques, mechanical loads need to be applied to the structure. In the optical fibre sensing systems, the possibility of failures in the wiring network, manufacturing and installation costs are some of the factors that should be paid attention to. Piezoelectric transducers used in the guided wave-based techniques should be attached on the surface of the structure under test. And before the DIC measurement, the sample surface should be speckled with black and white paints, which is not practical for large structures.

An alternative detection method is the microwave-based techniques. Microwaves can propagate in air and dielectric materials with low attenuation. There are a number of attributes when applying microwave testing, such as non-contact, no need for couplants or transducers bonded on the surface, operator friendly, relatively inexpensive and one-sided scanning [5–8]. Safety precautions are usually not necessary, as the signal power used is relatively low (few mW). In recognition of the growing interest in this technique, in 2014 the Microwave Testing Committee was established by the American Society for Non-destructive Testing (ASNT), and microwave testing was recognised as its own NDT method in the 2016 edition of the ASNT standards.

The existing microwave testing methods for CFRP composites can be categorised into five groups: self-sensing methods, near-field induction methods, near-field resonance methods, far-field methods and combination with other NDT methods [9]. Among these methods, the near-field resonance approach using a complementary split-ring resonator (CSRR) has attracted much attention in recent years, due to the distinct advantages of compact size, low cost, design simplicity, high sensitivity,

[*] College of Automation Engineering, Nanjing University of Aeronautics and Astronautics, Nanjing, 211106, China, [**] Nondestructive Detection and Monitoring Technology for High Speed Transportation Facilities, Key Laboratory of Ministry of Industry and Information Technology, Nanjing 211106, China, [***] Department of Electrical and Electronic Engineering, The University of Manchester, Manchester, M13 9PL, UK, [****] School of Mechanical Engineering, Hebei University of Technology, Tianjin 300130, China, zhenli@nuaa.edu.cn

DOI: 10.2478/jee-2019–0083, Print (till 2015) ISSN 1335-3632, On-line ISSN 1339-309X

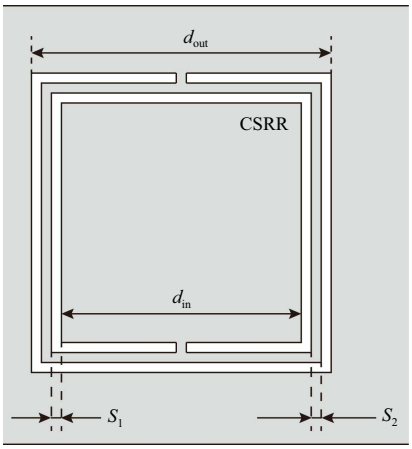

Fig. 1. General CSRR structure

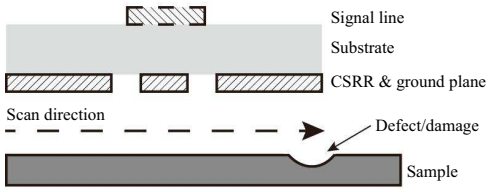

Fig. 2. Scan with a CSRR sensor for damage detection

easy fabrication and simple operation. This type of sensor has been introduced for permittivity measurement [10–12], thickness determination [13], detection of cracks in an aluminium plate [14, 15] and fibreglass materials [16]. However, so far little work has been done on its detection capabilities for carbon fibre composites.

In the present work, the applicability of the CSRR configuration for detection of impact damage in carbon fibre composites is explored. First, the sensing principle of the CSRR is explained. Then, design of a CSRR sensor is presented. The detection performance is examined by electromagnetic simulation, and the effect of the size of the impacted region on the resonant responses is studied. An experiment is conducted with an impacted CFRP sample to show the effectiveness of the sensor.

2 Sensing principle of a near-field CSRR sensor

Structure of a complementary split-ring resonator is shown in Fig. 1, which has a centre 'island' surrounded by a conducting plane that connects by two narrow bridges. From the equivalent lumped circuit point of view, the circuit consists of tightly distributed inductance and parasitic capacitance between the conductive traces. At resonance, the electric and magnetic fields exist not only in the space between the traces, but also in the surrounding (*ie* the fringe fields), which form a resonant system. The corresponding resonance frequency can be expressed as [17]

$$f_0 = \frac{1}{2\pi\sqrt{L_{\mathrm{eq}}C_{\mathrm{eq}}}} \tag{1}$$

where L_{eq} and C_{eq} are the equivalent inductance and capacitance, respectively.

The planar structure can be made on the ground plane of a microstrip line, which produces electric fields perpendicular to the resonator and consequently provides signal excitation. A schematic diagram of the scanning process is illustrated in Fig. 2, where the sensor is placed close to the sample so that any variation of the material properties and surface profile can affect the fringe fields. It is indicated that the CSRR sensing is a kind of near-field detection technique. When the sensor moves to an impacted region, the shape of the resonant fields is perturbed, resulting in a change in the resonance frequency. The resonance frequency shift can then be used as a damage indicator. Using the perturbation theory, the resonant frequency change can be estimated, assuming the perturbation is small, and the electromagnetic distribution remains the same [18]

$$\frac{f - f_0}{f_0} \approx \frac{\int_{\Delta\Gamma}(\mu|\overline{H}_0|^2 - \varepsilon|\overline{E}_0|^2)\mathrm{d}v}{\int_{\Gamma_0}(\mu|\overline{H}_0|^2 + \varepsilon|\overline{E}_0|^2)\mathrm{d}v} \tag{2}$$

where f is the resonant frequency after perturbation. μ and ϵ are the magnetic permeability and electric permittivity, respectively, and $|\overline{E}_0|$ and $|\overline{H}_0|$ are the original electric and magnetic fields, respectively. Here, V_0 is the original volume of the resonant region around CSRR, and ΔV is the volume changed. It is indicated that the resonance frequency may either increase or decrease, depending on the location of the perturbation and whether the original volume is enlarged or reduced.

3 Design of a CSRR sensor

Here in the design, the CSRR is made on a printed circuit board (PCB), and the PCB fabrication technique is adopted. The substrate of the PCB used is FR4, the dielectric constant (ε_r) and dielectric loss tangent of which are 4.8 and 0.017, respectively. The thickness of the substrate (t) is approximately 1.5 mm, and the thickness of the copper coating is $35\,\mu$m. For impedance matching, the width of the signal line (w) is designed to achieve the same characteristic impedance (*ie* $50\,\Omega$) as that of the SMA (Sub Miniature Version A) connector (for signal input and output). The characteristic impedance of the microstrip line Z can be calculated as [19]

$$Z = \begin{cases} \frac{60}{\sqrt{\varepsilon_{\mathrm{e}}}}\ln\left(\frac{8t}{w} + \frac{w}{4t}\right) & \text{for } w/t \le 1\,, \\ \frac{120\pi}{\sqrt{\varepsilon_{\mathrm{e}}}[w/t + 1.393 + 0.667\ln(w/t + 1.444)]} & \text{for } w/t \ge 1 \end{cases} \tag{3}$$

where ε_{e} is the effective dielectric constant, which is a function of ε_{r}, t and w.

$$\varepsilon_{\mathrm{e}} = \frac{\varepsilon_{\mathrm{r}} + 1}{2} + \frac{\varepsilon_{\mathrm{r}} - 1}{2}\frac{1}{\sqrt{1 + 12t/w}}\,. \tag{4}$$

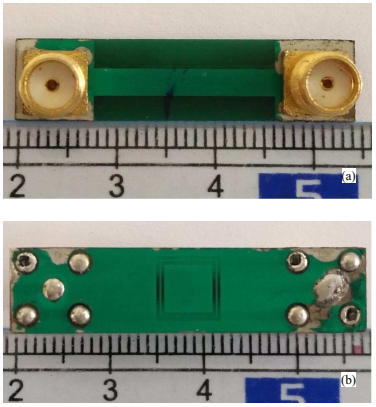

Fig. 3. Photographs of the CSRR sensor designed: (a) – upper side, (b) – lower side

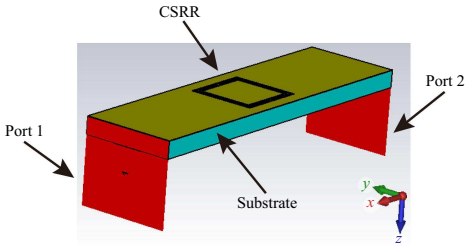

Fig. 4. Electromagnetic simulation model for the CSRR sensor designed

Hence, the width w is set to 2.8 mm. The values of the parameters related to the CSRR structure (Fig. 1) are listed in Tab. 1. The photographs of the CSRR sensor developed are presented in Fig. 3. On both sides there are thin green solder masks made of polymer for protection against oxidation.

4 Electromagnetic simulation

The performance of the CSRR sensor is evaluated using electromagnetic simulation software CST Microwave Studio. The model built is shown in Fig. 4. The strip line is 30 mm long, and the width of the PCB is 8.4 mm. The frequency domain solver is employed here for this electrically small structure. Based on the exponential fitting function given in [16], the resonance frequency of the resonator designed can be around 3.7 GHz, so a frequency range from 2 GHz to 4 GHz is used in the modelling.

The resonant response with air surrounding is presented in Fig. 5, which shows that the resonance frequency is around 2.5634 GHz and the minimum attenuation reaches −54.78 dB. Hence, in the simulation cases followed, a frequency range of 2–3 GHz is adopted for better description and quicker computation. The difference between the resonance frequency given by the estimation and simulation is primarily due to the fact that the empirical expression in [16] is only suited to the Rogers RO4350 substrate, while it can still be used as an initial guess for the frequency range setting in the simulation.

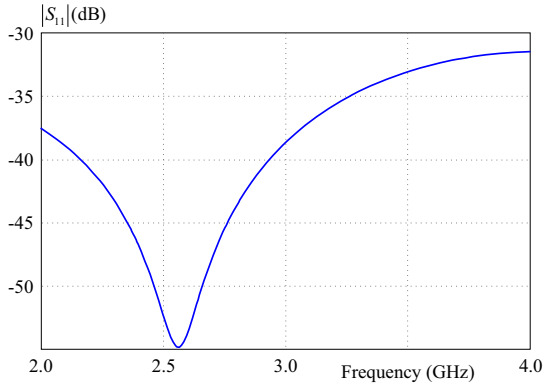

Fig. 5. Resonant response of the CSRR sensor with air surrounding simulated over 2–4 GHz

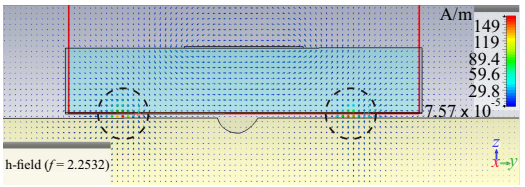

Fig. 6. Resonant magnetic field distribution around the sensor over a dent modelled

Then, a composite plate is incorporated in the model. The distance between the sample and the sensor (*ie* standoff distance) is set to 0.1 mm. The composite is assumed homogeneous, and permittivity of 46–j15 [20] is adopted over the frequency range investigated. In addition, a half-sphere dent with a radius of 0.5 mm is created in the top surface of the sample to simulate impact damage. In the present case the resonance frequency is shifted downwards to 2.2532 GHz, which is mainly due to the increased capacitance around the resonator. The resonant magnetic field in the cross-sectional plane perpendicular to the feed line at the centre is shown in Fig. 6, where the maximum magnitudes exist at the short traces (black circled) connecting the inner conductor to the outer ground plane. Hence, it is suggested that optimal sensitivity can be achieved when the impacted region is placed under the narrow traces.

Parametric study is conducted to assess the effect of the damage size on the resonance frequency. As seen in Tab. 2, the resonance frequency is increased with increasing dent size. This trend is what can be expected according to the prediction by (2). It is also indicated

Table 1. Dimensions of the CSRR structure

Diameter of the inner conductor (d_{in} mm)	Diameter of the whole resonator (d_{out} mm)	Spacing between the trace and inner conductor (s_1 mm)	Trace width (s_2 mm)
4.8	6.0	0.2	0.2

Table 2. Comparison of the resonance frequency for different sizes of the dent simulated

Radius of the dent (r_{d}, mm)	0.4	0.5	1.0	1.5	2.0
Resonance frequency (f, MHz)	2245.0	2253.2	2258.6	2266.6	2296.4

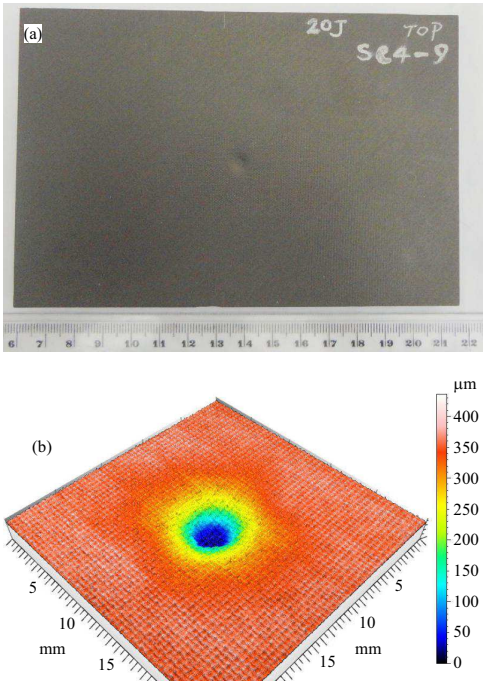

Fig. 7. A composite sample with barely visible impact damage under test: (a) – photograph, (b) – 3D view of the impact image by chromatic confocal optical microscopy

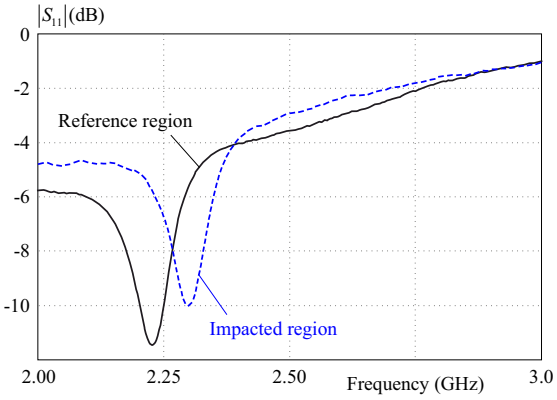

Fig. 8. Frequency responses of the CSRR sensor for impact damage detection

that the frequency shift is larger for a higher dent size, *eg* a 43.2 MHz difference between $r_d = 0.5$ mm and $r_d = 2.0$ mm.

5 Experiments

The developed CSRR sensor was applied to detect impact damage in the top surface of a 4 mm thick composite panel shown in Fig. 7(a). This kind of damage, categorised as barely visible impact damage (BVID), was created by a drop-weight impact energy of 20 J. The diameter and depth of the dent observed by an optical microscope were approximately 3.85 mm and 340 μm, respectively. In addition, a detailed three-dimensional view of the impact damage was produced by chromatic confocal optical microscopy. For the PS4D optical pen used, a height range up to 3 mm and a vertical resolution of 40 nm can be achieved. An acquisition rate of 2000 Hz and a step size of 10 μm $\times$ 50μm were utilised. The image obtained is shown in Fig. 7(b). It was revealed that the area of the impacted surface was 201.4 mm^2 and the maximum depth of the dent was 356.4 μm.

In the test, the CSRR sensor was connected to a HP 8510C Vector Network Analyser (VNA) with two coaxial cables. A personal computer was connected to the analyser by an IEEE-488 cable. A MATLAB® programme was developed for data acquisition. The measurement was done over 2–3 GHz with 201 frequency points. Point scanning was performed above the sample with a standoff distance of 100 μm. First, the location without impact damage underneath was measured as a reference; then, the impacted region was measured for comparison. The results are presented in Fig. 8, where the curve patterns are in good agreement with the simulation (Fig. 5) though the permittivity values of the materials studied are different. Similarly, the resonance frequency is shifted upwards when the CSRR sensor is moved to the damaged region. The variation of the resonance frequency and quality factor (or Q factor) due to the existence of the impact damage are listed in Tab. 3.

Table 3. Changes in the resonance frequency and Q factor due to the impact damage

	Intact region	Impacted region
f_{R} (MHz)	2230.0	2295.0
Q factor	31.86	28.69

6 Concluding remarks

A novel approach for detection of impact damage in CFRP composites using a complementary split-ring resonator sensor has been demonstrated. During inspection, the resonator, the conductive composite material and the air space in between comprise a resonant region. When a dent produced by impact damage is in the near field of the sensor, the damage induces shape perturbation, resulting in resonance frequency change.

The design of a CSRR sensor developed has been described in detail. And electromagnetic simulation has been conducted, where a more accurate approximation of

the resonant frequency is obtained, and the most sensitive sensing element is found. In addition, parametric study has been carried out to evaluate the effect of the damage size on the variation of the resonant frequency. It has been demonstrated that the larger the damage, the more variations it will cause, which is advantageous for practical applications. Detection of a barely visible impact damage in a composite plate was performed. An increase of 65 MHz in the resonance frequency and a decrease in the Q factor have been revealed. The proposed sensor can be extended to inspection of three-dimensional surfaces, where a flexible PCB substrate can be chosen.

Acknowledgements

This work was financially supported by NUAA research fund (YAH18097), Shuangchuang Project of Jiangsu Province (China) and MIIT Key Laboratory of nondestructive detection and monitoring technology for high speed transportation facilities (China). The first author gratefully acknowledges valuable discussions with Dr. Muhammad Firdaus. Special thanks to Andrea Novitsky from Nanovea and Mark Shropshall from Mi-Net Technology (UK and Ireland distributor) for their help in chromatic confocal optical microscopy.

References

[1] C. Soutis, "Carbon Fiber Reinforced Plastics in Aircraft Construction", *Mater. Sci. Eng. A,* vol. 412, no. 1–2, pp. 171–176, Dec 2005.

[2] K. Diamanti, J. M. Hodgkinson, and C. Soutis, "Detection of Low-Velocity Impact Damage in Composite Plates using Lamb Waves", *Struct. Heal. Monit.* vol. 3, no. 1, pp. 33–41, Mar 2004.

[3] B. Keshtegar, P. Hao, Y. Wang, and Y. Li, "Optimum Design of Aircraft Panels Based on Adaptive Dynamic Harmony Search", *Thin-Walled Struct.*, vol. 118, pp. 37–45, 2017.

[4] Z. Li, A. Haigh, C. Soutis, A. Gibson, and R. Sloan, "Applications of Microwave Techniques for Aerospace Composites", *2017 IEEE International Conference on Microwaves, Antennas, Communications Electronic Systems* (COMCAS), pp. 1–4, Nov 2017.

[5] S. Kharkovsky and R. Zoughi, "Microwave Millimeter Wave Nondestructive Testing Evaluation – Overview Recent Advances", *IEEE Instrum. Meas. Mag.* vol. 10, no. 2, pp. 26–38, Apr 2007.

[6] J. T. Case and S. Kenderian, "Microwave NDT: An Inspection Method", *Mater. Eval.* vol. 75, no. 3, pp. 339–346, 2017.

[7] Z. Li, A. Haigh, C. Soutis, and A. Gibson, "Principles Applications of Microwave Testing for Woven Non-Woven Carbon Fibre-Reinforced Polymer Composites: a Topical Review", *Appl. Compos. Mater.* vol. 25, no. 4, pp. 965–982, Aug 2018.

[8] Z. Li, A. Haigh, C. Soutis, A. Gibson, and P. Wang, "A Review of Microwave Testing of Glass Fibre-Reinforced Polymer Composites", *Nondestruct. Test. Eval.* vol. 34, no. 4, pp. 429–458, Oct 2019.

[9] Z. Li, "Radio Frequency Non-Destructive Evaluation of Impact Damage in Carbon Fibre Composites", *University of Manchester* 2017.

[10] S. Lee and C. L. Yang, "Complementary Split-Ring Resonators for Measuring Dielectric Constants Loss Tangents", *IEEE Microw. Wirel. Components Lett.* vol. 24, no. 8, pp. 563–565, Aug 2014.

[11] X. Zhang, C. Ruan, T. Haq, and K. Chen, "High-Sensitivity Microwave Sensor for Liquid Characterization Using a Complementary Circular Spiral Resonator", *Sensors*, vol. 19, no. 4, p. 787, Feb 2019.

[12] M. A. H. Ansari, A. K. Jha, and M. J. Akhtar, "Design Application of the CSRR-Based Planar Sensor for Noninvasive Measurement of Complex Permittivity", *IEEE Sens. J.* vol. 15, no. 12, pp. 7181–7189, 2015.

[13] M. S. Boybay and O. M. Ramahi, "Non-Destructive Thickness Measurement using Quasi-Static Resonators", *IEEE Microw. Wirel. Components Lett.* vol. 23, no. 4, pp. 217–219, Apr 2013.

[14] A. M. Albishi, M. S. Boybay, and O. M. Ramahi, "Complementary Split-Ring Resonator for Crack Detection in Metallic Surfaces", *IEEE Microw. Wirel. Components Lett.* vol. 22, no. 6, pp. 330–332, Jun 2012.

[15] A. Ali, M. El Badawe, and O. M. Ramahi, "Microwave Imaging of Subsurface Flaws in Coated Metallic Structures Using Complementary Split-Ring Resonators", *IEEE Sens. J.* vol. 16, no. 18, pp. 6890–6898, Sep 2016.

[16] A. Albishi and O. M. Ramahi, "Detection of Surface Subsurface Cracks in Metallic Non-Metallic Materials using a Complementary Split-Ring Resonator", *Sensors* (Switzerland), vol. 14, no. 10, pp. 19354–19370, Jan 2014.

[17] J. B. Marion, W. F. Hornyak, *Physics for Science Engineering*, Saunders College 1982.

[18] D. M. Pozar, "Microwave Engineering", Fourth edition, New York: John Wiley & Sons, 2012.

[19] B. C. Wadell, *Transmission Line Design Handbook*, Massachusetts: Artech House, 1991.

[20] M. Y. Koledintseva, J. Drewniak, R. Dubroff, K. Rozanov, and B. Archambeault, "Modeling of Shielding Composite Materials Structures F0R Microwave Frequencies", *Prog. Electromagn. Res. B*, vol. 15, pp. 197–215, 2009.

Received 15 October 2019

Zhen Li (Assoc Prof, PhD) received the BEng. degree from Nanjing University of Aeronautics and Astronautics (NUAA) and MEng. degree from Shanghai Jiao Tong University (SJTU), China, in 2010 and 2013, respectively, and the PhD degree from The University of Manchester, UK, in 2017. He is currently an Associate Professor with College of Automation Engineering, NUAA. He has authored and coauthored over 20 technical peer-reviewed papers in international journals and conference proceedings. His research interests include non-destructive testing of fibre-reinforced polymer composite materials and microwave testing.

Arthur Haigh (PhD) was born in Scarborough, North Yorkshire, United Kingdom (UK). He received the PhD degree from Manchester Metropolitan University, UK, in 1994. He is currently a Visiting Research Fellow with Department of Electrical and Electronic Engineering, The University of Manchester, UK. His industrial career was principally with Ferranti Ltd (UK). For the last nine years of his industrial career, he was with the Microelectronics Centre, responsible for the introduction of direct step-on-wafer lithography machines. As the Special Projects Manager, he managed the technical side of an ESPRIT II proposal involving 14 other European companies and a total budget of 30 million pounds. He left the industry in 1988, and for three years, he taught physics at Manchester Metropolitan University.